Effect of gold intercalation on the electronic structure of graphene on Co−Si/SiC(0001)

© A.A. Rybkina, S.O. Filnov, D.A. Glazkova, O.Yu. Vilkov, K.A. Bokai, D.A. Pudikov, A.M. Shikin, A.G. Rybkin

St. Petersburg State University,
St. Petersburg, Russia

E-mail: a.rybkina@spbu.ru

Graphene grown on an ultrathin $CoSi/CoSi_2$ silicide layer atop a SiC(0001) substrate and intercalated by Au was studied. Intercalation of Au was found to occur at a temperature of $500°C$, and it is accompanied by the formation of gold silicide under graphene with a stoichiometry close to Au_2Si. The study of the electronic structure of the system in the region of the $\overline{K}$ point of the surface Brillouin zone revealed the quasi-freestanding character of graphene with a linear spectrum of π states and a Dirac point near the Fermi level. Photoelectron microscopy revealed the homogeneity of the work function along the surface of the sample on a micrometer scale.

1. Introduction

Graphene is one of the promising materials for use in post-silicon electronics and spintronics [1–3]. Linear law of electron states dispersion in graphene provides high mobility of charge carriers and dissipativeless electron transport. Being a non-magnet material with weak spin-orbital interaction, graphene could not be considered as an active element of spintronics. However, giant spin splitting of electron states observed in graphene placed in contact with heavy and magnetic metals at room temperature opens wide prospects for its use in spintronics devices, in particular, in the field of data storage and quantum calculations [4–9]. One of the promising implementation of graphene in spintronics is magneto-spin-orbit graphene [10], which is well ordered graphene in contact with strong ferromagnet (cobalt) and heavy metal (gold). When interacting with cobalt and gold, graphene not only preserves its unique characteristics, but partially borrows properties of these metals — magnetism and spin-orbit interaction. For transport measurements on magneto-spin-orbit graphene, our primary objective was to synthesize such graphene on an insulating substrate. Therefore, implementation of magneto-spin-orbit graphene on semiconductor single crystal substrate SiC(0001) is a quite expected and rather relevant task. Besides, combination of strong spin-orbit interaction and magnetism in graphene-derived system on SiC may become a promising platform for observation of quantum abnormal Hall effect in graphene (QAHE) [11,12].

To solve this task, we at first intercalated Co atoms under a buffer layer of graphene on substrate $6H$-SiC(0001) [13,14]. Buffer layer is a graphene-like surface layer with $(6\sqrt{3} \times 6\sqrt{3}))R30$ reconstruction, which forms in the process of annealing and graphitization of SiC single crystal [15,16]. Intercalation of cobalt under the buffer layer turns it into graphene monolayer. As a result quasi-freestanding, one-atom-thick graphene was formed on magnetic ultrathin layer of cobalt silicides with stoichiometry close to $CoSi/CoSi_2$. Ferromagnetic ordering was found along the surface, provided for by CoSi layer under graphene.

The next step toward the synthesis and investigation of magneto-spin-orbit graphene on semi-insulating substrate was made in this work. The subsequent intercalation of Au atoms into the graphene/CoSi/$CoSi_2$/SiC(0001) system was performed. As it is known, intercalation of gold under graphene on metal surfaces Co(0001), Ni(111) [8–10,17] and non-metal substrates [18] induces spin-orbit interaction in graphene and giant spin-splitting of electron π states of graphene in the area of the Dirac point. It is expected that gold intercalation will enhance spin-orbital interaction in the investigated system and will modify its electronic and spin structure. This work seems to be an important step in the way towards the creation of magneto-spin-orbit graphene on semiconducting substrate, and the results obtained can be useful for further investigation of electronic spin structure and transport properties of the synthesized system.

2. Research methods

Synthesis of the sample and preliminary photoemission studies were carried out *in situ* under ultrahigh vacuum conditions on photoelectron spectrometer „Univer-M" at the Resource Center „Physical Methods of Surface Inves-

tigation" (RC PMSI) of Saint Petersburg State University Research park. The *n*-type and semi-insulating wafers of 6*H*-SiC(0001) purchased from TankeBlue Semiconductor Co. Ltd. were used for synthesis. The thickness of deposited gold layers was monitored using a quartz microbalance. Annealing temperature was determined using pyrometer Keller CellaTemp PA 20 AF 2/C. Studies by angle-resolved photoelectron spectroscopy method (ARPES) were performed at room temperature in RC PMSI on a unique scientific platform „Nanolab", which is equipped with hemispherical energy analyzer VG Scienta R4000 with a microchannel detector and narrowband high intensity source of ultraviolet radiation with monochromator. Studies by method of photoelectron spectroscopy of core levels with high resolution (XPS) were performed at room temperature at station RG-PES in Russian-German beamline in the center of synchrotron radiation Helmholtz-Zentrum Berlin für Materialien und Energie (BESSY II). Calibration of measured XPS spectra was carried out by position of the Fermi level. The photoelectron spectra of the core levels were deconvoluted into spectral components by fitting procedure. The line shape of spectra was defined by asymmetric Gaussian/Lorentzian product formula [19,20]. The graphene peak asymmetry parameter in spectra C 1*s* was 0.08. Experimental data points of spectra were shown in figures by a line with round markers together with results of deconvolution into components and background. Measurements using photoelectron microscopy (PEEM) were carried out using station Omicron FOCUS IS-PEEM in the center of synchrotron radiation BESSY II. A source of photons was a gas discharge Hg lamp ($h\nu = 4.9$ eV).

3. Results and discussion

This work performed intercalation of gold atoms by deposition of a film with thickness of 3.2 Å on previously degassed and characterized surface of graphene/CoSi/CoSi$_2$/SiC system. After this the system was annealed at 450°C and 500°C for 15 min at each temperature.

Fig. 1 shows a survey photoelectron spectrum for the system received after deposition of Au and annealing at $T = 500$°C. In the spectrum, apart from carbon, silicon and cobalt peaks, gold peaks appeared. Small oxygen peak was present in the initial system as well and is possibly related to transfer of sample in pre-vacuum conditions.

Detailed analysis of photoelectron spectra in the region of C 1*s*-, Si 2*p*-, Au 4*f*-, Co 2*p*-levels after deposition of Au and annealing of the system at $T = 500$°C was carried out. Photoelectron spectra were measured at two values of photon energy — 420 eV for increase of surface sensitivity and 980 eV for elementary analysis. Measurements at photon energy 420 eV differ with higher intensity of photon flux on the synchrotron radiation beamline. However, the length of free path of excited photoelectrons turns out to be less than when using excitation energy 980 eV. In connection with this, in spectra C 1*s*-signal from underlying substrate SiC is
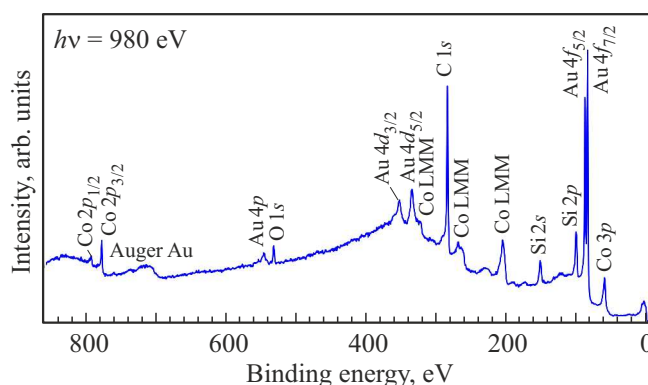
Figure 1. Survey XPS-spectrum of core levels for the system after deposition of gold and annealing at $T = 500$°C, measured with the photon energy 980 eV. The spectrum includes the main spectral lines specific for carbon, silicon, gold and cobalt atoms.

too low. Besides, the photon energy 420 eV is not sufficient to measure range of energies compliant with level Co 2*p*. Therefore, for analysis of full set of XPS-spectra, including spectra C 1*s* and Co 2*p*, measurements were carried out at photon energy 980 eV.

Fig. 2 shows XPS-spectra measured normally to the surface in the region of C 1*s*-, Si 2*p*-, Au 4*f*-levels using the photon energy 420 eV.

The C 1*s* spectrum after deposition of Au and annealing of the system (Fig. 2, *a*) represents a single-component asymmetric peak at the binding energy of 284.3 eV, which is 0.1 eV lower than carbon atom binding energy in graphene before Au deposition [13]. The Si 2*p* spectrum, shown in Fig. 2, *b*, has a complex multi-component structure. In order to identify each of components, it is necessary to refer to the analysis of Si 2*p* spectrum before deposition of Au. The paper [13] demonstrated that cobalt intercalation under graphene buffer layer leds to appearance of two new components on the left and on the right of the main peak in spectrum of Si 2*p*. Component at lower binding energy (-1.45 eV) complies with compound CoSi$_2$, and at higher binding energy ($+1.05$ eV) complies with compound CoSi. After deposition of Au and annealing of the system, an additional component appeared in the Si 2*p* spectrum at the binding energy of 102.87 eV (energy is specified for Si 2*p*$_{3/2}$), see Fig. 2, *b*. Analysis of the Au 4*f* spectrum on Fig. 2, *c*, measured with higher energy resolution, shows that the system is characterized by gold atoms in two states. Each of Au 4*f* doublet lines consists of two components. The high energy components of Au 4*f*$_{7/2}$ and Au 4*f*$_{5/2}$ at the binding energies of 84 and 87.6 eV correspond to the gold atoms in metal state. These atoms presumably are located on the graphene surface and are not intercalated under graphene monolayer. The low energy pair of components shifted by 0.28 eV, i.e. at the binding energies of 87.32 and 83.72 eV corresponds to the gold atoms which interact with the substrate to form a chemical bond.
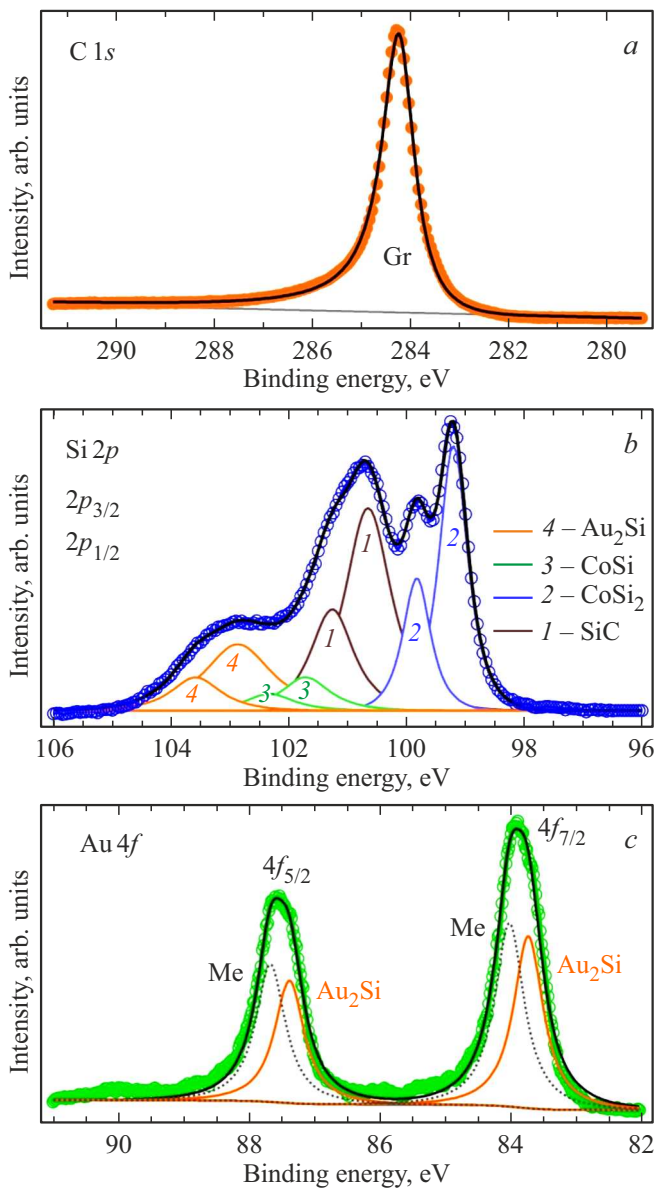
Figure 2. Photoelectron spectra of C $1s$, Si $2p$, Au $4f$ with high resolution measured normally to the surface. Photon energy is 420 eV.

The results of the fitting procedure for Si $2p$ and Au $4f$ spectra measured with photon energy 420 eV were used to analyze XPS-spectra at 980 eV. Fig. 3 shows photoelectron spectra measured at photon energy of 980 eV in the region of C $1s$, Si $2p$, Au $4f$ and Co $2p$ core levels. The C $1s$ spectrum in Fig. 3, a has a distinctive line shape for graphene on SiC [15,16,21,22]: peak corresponding to carbon atoms in graphene has the binding energy of 284.3 eV, and peak corresponding to carbon in SiC volume has bond energy 282.9 eV. When the photon energy is 980 eV, it is possible to differentiate a signal not only from graphene layer, but from SiC substrate in the carbon spectrum, which is significant for further analysis of photoelectron spectra. Spectrum of Si $2p$ in Fig. 3, b also has multi-component form as in

Fig. 2, b, however, individual doublets of spectral lines are resolved worse. Therefore, it was important to analyze the set of photoelectron spectra measured at different photon energies. The spectrum of Co $2p_{3/2}$, shown in Fig. 3, c, consists of the main component with the binding energy of 778.15 eV and the satellite peak from high energy side. And, finally, the spectrum of Au $4f$ in Fig. 3, d is a doublet similar to the spectrum in Fig. 2, c. Besides, intensity of components from the gold atoms interacting with the substrate significantly exceeds the signal from the gold atoms in metal state.

By ratio of signal intensities from interacting atoms in spectra of Au $4f$ and Si $2p$, it is possible to assess ratio of gold and silicon atoms as 2 : 1. This correlates with the literature data on deposition of gold films on the silicon substrate [23–27], which show that when the gold films are deposited with thickness above 2 Å, the structural realignment of the interface takes place, which is accompanied by break of Si−Si bonds, formation of chemical bonds between Si and Au atoms and formation of region with mutual silicon and gold interdiffusion.

Therefore, one may conclude that in the interface between graphene and substrate a transition layer is formed, where gold and silicon atoms are mixed, and silicide with stoichiometry Au_2Si originates.

Photoelectron spectra using the photon energy of 980 eV were measured at various photoelectron emission angles — normally to the surface $(0°)$ and at angle $60°$ relative to the surface normal. Then each of these spectra was deconvoluted into spectral components, and component intensities were determined as areas under curves. Intensity of the component measured at angle $60°$, referred to intensity of the component, measured along the surface normal, gives us the ratio of intensities $I(60°)/I(0°)$, presented in the Table. Such ratio makes it possible to analyze elementary and chemical composition of the sample depending on depth. The lower the ratio $I(60°)/I(0°)$, the deeper (further from the surface) is the element and the compound, where it is located. Based on the taken results we conclude that graphene is the top layer of the system. Besides, immediately under graphene there is gold silicide formed, close in stoichiometry to Au_2Si, cobalt silicides

Ratio of intensities of certain photoelectron spectra components as a result of measurement at two angles of photoelectron emission — $0°$ and $60°$

Name of Compound	Reference Peak	Binding energy, eV	$I(60°)/I(0°)$
Graphene	C $1s$	284.3	0.23
Au_2Si	Au $4f_{7/2}$	83.72	0.21
Au_2Si	Si $2p_{3/2}$	102.87	0.20
CoSi	Si $2p_{3/2}$	101.7	0.12
$CoSi_2$	Si $2p_{3/2}$	99.2	0.096
$CoSi_2$	Co $2p_{3/2}$	778.15	0.096
SiC bulk	Si $2p_{3/2}$	100.65	0.055
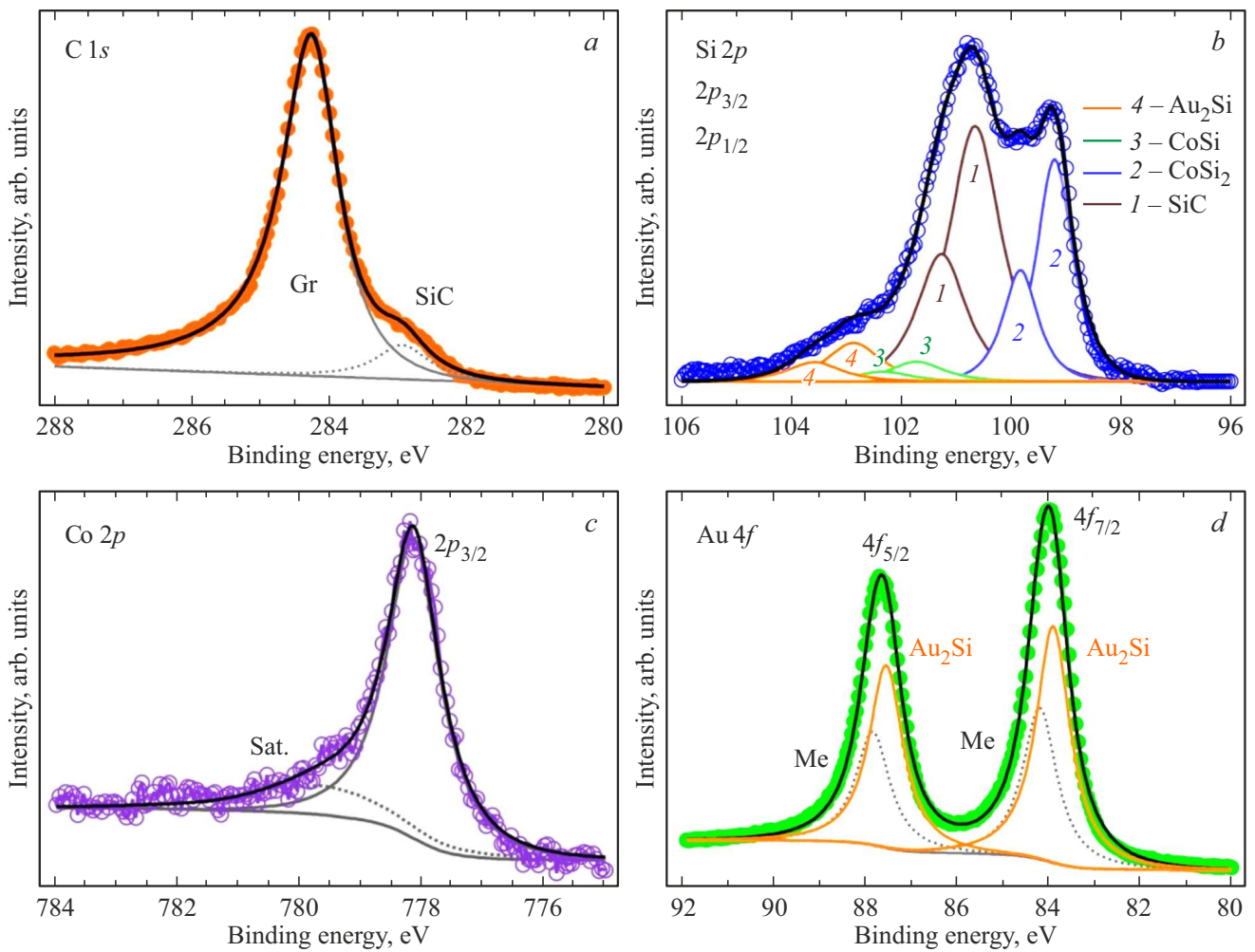
Figure 3. Photoelectron spectra C $1s$, Si $2p$, Co $2p_{3/2}$, Au $4f$, measured normally to surface. Photon energy 980 eV.
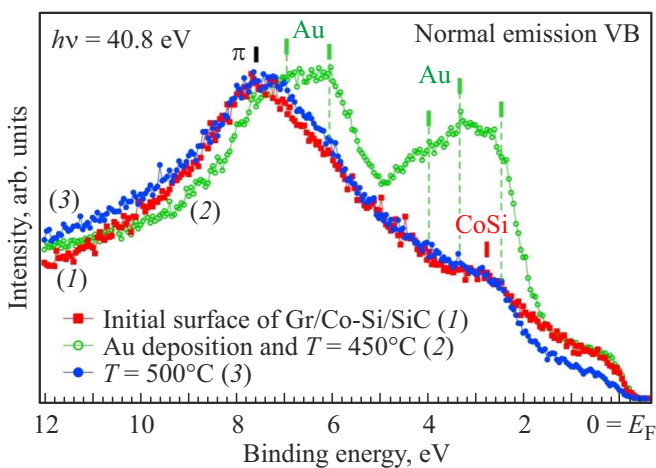
Figure 4. Photoelectron spectra of the valence band for initial surface graphene/CoSi/CoSi$_2$/SiC — (1), and also after deposition of gold and annealing of the system at $T = 450°$C — (2) and $T = 500°$C — (3). Spectra are measured normally to the surface and at photon energy of 40.8 eV.

CoSi and CoSi$_2$ are located even deeper, and SiC silicon carbide substrate lies in the base. These data confirms that synthesis led to intercalation of gold atoms under graphene monolayer to form a transition layer that contains gold silicide Au$_2$Si.

Let us consider the changes in electron structure of the valence band after Au intercalation. Fig. 4 shows change of photoelectron spectra of the valence band in process of the system formation. After gold deposition on the surface of graphene/CoSi/CoSi$_2$/SiC system and annealing at $T = 450°$C (green spectrum (2)), contribution of $5d$-gold states [17] appears in the spectrum, intensity of graphene π states drops significantly at the same time, and spectrum shape near the Fermi level remains practically same.

Further annealing of the system at $T = 500°$C (blue spectrum (3)) results in significant reduction of intensity of $5d$-band Au signal, but contribution of gold states at the energy regions 2.5−4.5 and 6−7 eV remains. Besides, signal intensity is restored for π states of graphene at the energy of 7.6 eV, and spectrum shape changes near the Fermi level in the region from 0 to 2 eV. In paper [23] it
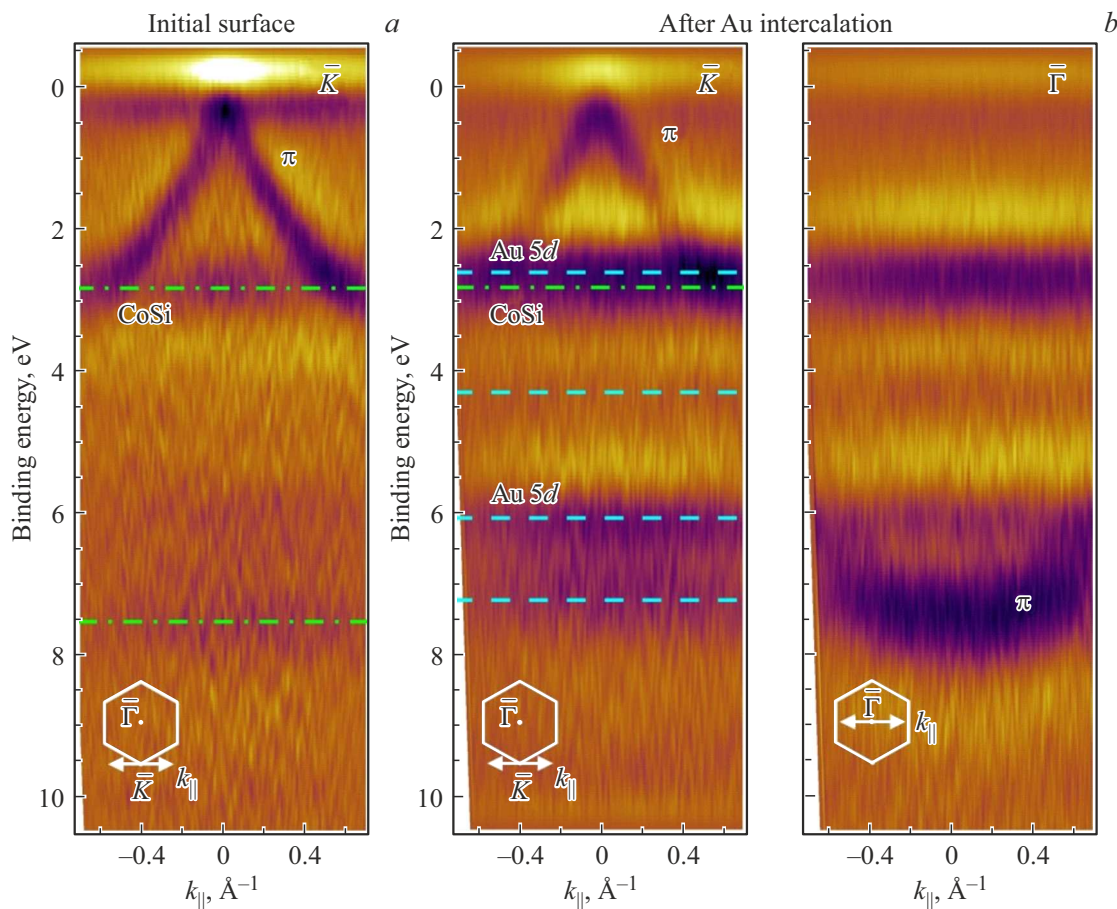
Figure 5. Dispersion dependences of the electron states of the formed system after Au intercalation measured in the area of $\overline{K}$ and $\overline{\Gamma}$ points of graphene Brillouin zone. ARPES-intensity maps are measured in the direction perpendicular to the $\overline{\Gamma K}$ direction of the Brillouin zone, measurement direction is schematically shown on figures in the bottom left corner. Photon energy is 40.8 eV. Green dash-dot lines on the figure show CoSi states, and blue dotted lines — 5d-states of Au.

was shown that when thin film of gold is deposited on the silicon substrate, the spectral intensity near the Fermi level is noticeably lower than for metal gold, which is explained by valence band realignment when gold silicide is formed. Such observations are illustrative of interaction between intercalated gold atoms with the substrate as a result of system heating to $T = 500°C$.

Dispersion dependences of the electron states in the area of $\overline{K}$ point of the surface Brillouin zone for graphene/CoSi/CoSi$_2$/SiC initial system are shown in Fig. 5 (a). Electron π states of graphene have linear nature $E(k)$ of dependence and form the Dirac cone, specific for graphene. And the Dirac point is localized near the Fermi level.

Apart from graphene states, the electron structure includes non-dispersing flat bands at 2.8 and 7.5 eV, which may be related to CoSi compound, according to the theoretical calculations of the bulk density of states [28] and experimental ARPES-data [29]. Besides, calculations of the band structure of graphene on CoSi in paper [14], demonstrated availability of such states at the binding energy around 2.8 eV.

After intercalation of Au, the electron structure is modified in the area of $\overline{K}$ and $\overline{\Gamma}$ points (Fig. 5, b). In the area of binding energies from 2.5 to 7.5 eV, 5d-gold states emerge. CoSi states at 2.8 eV still remains visible on spectra.
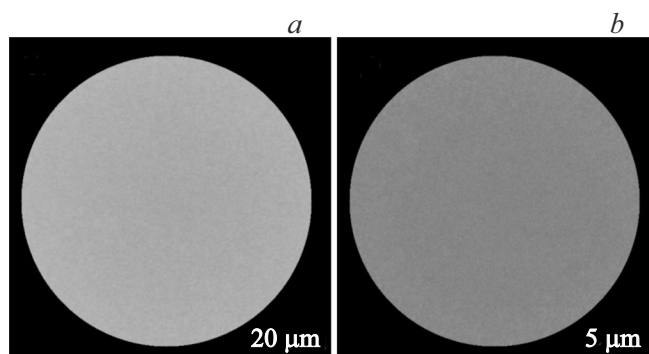
Figure 6. PEEM images acquired with a Hg discharge lamp as source of photons ($hv = 4.9$ eV) from areas with size 20 μm and 5 μm for visualization of sample surface homogeneity at different scale.

Bottom of π band of graphene is located at the binding energy of 7.5 eV (Fig. 5, *b*), while for graphene on SiC(0001) this value is ~ 8.5 eV [15], and for graphene on Ni(111) or Co(0001) after intercalation of Au — around 8 eV [8,9,30]. At the same time, the binding energy of C 1*s* graphene level in the studied system is also lower than in graphene on SiC(0001) (284.6 eV [31]), and turns out to be close to the binding energy of C 1*s* graphene level on Ni(111) after intercalation of Au (284.3 eV [30]). Energy position of C 1*s* level and position of bottom of π-graphene band in $\overline{\Gamma}$ point correlate with energy of graphene interaction with substrate. According to [30], the lower the energy of C 1*s* level and position of π band bottom, the lower the energy of graphene interaction with substrate.

Presented results in a combination with linear spectrum of π states in area of $\overline{K}$ point is illustrative of quasi-freestanding character of graphene and weak interaction of graphene with underlying substrate.

To visualize homogeneity of sample surface, measurements by photoelectron microscopy method (PEEM) were carried out. Fig. 6 shows PEEM-images of formed system surface at different scale. Contrast on PEEM images shows work function changes along the sample surface. PEEM data analysis demonstrated that surface was characterized by the same work function of 4.2 eV in all points of the sample, which is illustrative of the system surface homogeneity. Indeed, if gold intercalation was not even, there would be sections on the surface with different work function [32]. Therefore, at micrometer scale we can talk about homogeneity of the synthesized system surface.

4. Conclusion

The this work we studied intercalation of Au atoms under graphene formed on layer CoSi/CoSi$_2$ on substrate SiC(0001). Deposition of Au atoms and annealing of the system at $T = 500°$C leads to gold intercalation under graphene. Data of photoelectron spectroscopy is illustrative of interaction between intercalated Au atoms and substrate to form a transition layer, where gold and silicon atoms are mixed, and silicide with stoichiometry Au$_2$Si originates. Besides, π states of graphene preserve linear nature of a Dirac cone with the Dirac point localized near the Fermi level. Studies using photoelectron microscopy demonstrated homogeneity of work function along sample surface at micrometer scale. Reported results will serve as the basis to measure electron spin structure and transport characteristics of synthesized graphene-containing system after intercalation of Co and Au in order to further study of magneto-spin-orbit graphene.

Conflict of interest

The authors declare that they have no conflict of interest.

References

[1] W. Han, R.K. Kawakami, M. Gmitra, J. Fabian. Nature Nanotechnology **9**, 794 (2014).

[2] J.I-J. Wang, D. Rodan-Legrain, L. Bretheau, D.L. Campbell, B. Kannan, D. Kim, M. Kjaergaard, P. Krantz, G.O. Samach, F. Yan, J.L. Yoder, K. Watanabe, T. Taniguchi, T.P. Orlando, S. Gustavsson, P. Jarillo-Herrero, W.D. Oliver. Nature Nanotechnology **14**, 120 (2019).

[3] A. Avsar, T.-Y. Yang, S. Bae, J. Balakrishnan, F. Volmer, M. Jaiswal, Z. Yi, S. R. Ali, G. Güntherodt, B. H. Hong, B. Beschoten, B. Özyilmaz. Nano Lett. **11**, *6*, 2363 (2011).

[4] A.A. Rybkina, A.G. Rybkin, I. Klimovskikh, P.N. Skirdkov, K.A. Zvezdin, A.K. Zvezdin, A.M. Shikin. Nanotechnology **31**, 165201 (2020).

[5] A.M. Shikin, A.A. Rybkina, A.G. Rybkin, I.I. Klimovskikh, P.N. Skirdkov, K.A. Zvezdin, A.K. Zvezdin. Appl. Phys. Lett. **105**, 042407 (2014).

[6] A.A. Rybkina, A.G. Rybkin, V.K. Adamchuk, D. Marchenko, A. Varykhalov, J. Sánchez-Barriga, A.M. Shikin. Nanotechnology **24**, 295201 (2013).

[7] I.I. Klimovskikh, M.M. Otrokov, V.Yu. Voroshnin, D. Sostina, L. Petaccia, G. Di Santo, S. Thakur, E.V. Chulkov, A.M. Shikin. ACS Nano **11**, *1*, 368 (2017).

[8] D. Marchenko, A. Varykhalov, M.R. Scholz, G. Bihlmayer, E.I. Rashba, A. Rybkin, A.M. Shikin, O. Rader. Nature Commun. **3**, 1232 (2012).

[9] A.M. Shikin, A.G. Rybkin, D. Marchenko, A.A. Rybkina, M.R. Scholz, O. Rader, A. Varykhalov. New J. Phys. **15**, 013016 (2013).

[10] A.G. Rybkin, A.A. Rybkina, M.M. Otrokov, O.Yu. Vilkov, I.I. Klimovskikh, A.E. Petukhov, M.V. Filianina, V.Yu. Voroshnin, I.P. Rusinov, A. Ernst, A. Arnau, E.V. Chulkov, A.M. Shikin. Nano Lett. **18**, *3*, 1564 (2018).

[11] Z. Qiao, S.A. Yang, W. Feng, W.-K. Tse, J. Ding, Y. Yao, J. Wang, Q. Niu. Phys. Rev. B **82**, 161414(R) (2010).

[12] X. Deng, S. Qi, Y. Han, K. Zhang, X. Xu, Z. Qiao. Phys. Rev. B **95**, 121410(R) (2017).

[13] A.A. Rybkina, S.O. Filnov, A.V. Tarasov, D.V. Danilov, M.V. Likholetova, V.Yu. Voroshnin, D.A. Pudikov, D.A. Glazkova, A.V. Eryzhenkov, I.A. Eliseyev, V.Yu. Davydov, A.M. Shikin, A.G. Rybkin. Phys. Rev. B **104**, 155423 (2021).

[14] S.O. Filnov, A.A. Rybkina, A.V. Tarasov, A.V. Eryzhenkov, I.A. Eliseev, V.Yu. Davydov, A.M. Shikin, A.G. Rybkin. ZhETF **161**, *2*, 227 (2022) (in Russian).

[15] K.V. Emtsev, F. Speck, T. Seyller, L. Ley, J.D. Riley. Phys. Rev. B **77**, 155303 (2008).

[16] C. Riedl, C. Coletti, U. Starke. J. Phys. D **43**, 374009 (2010).

[17] A.M. Shikin, G.V. Prudnikova, V.K. Adamchuk, F. Moresco, K.-H. Rieder. Phys. Rev. B **62**, 13202 (2000).

[18] D. Marchenko, A. Varykhalov, J. Sánchez-Barriga, Th. Seyller, O. Rader. Appl. Phys. Lett. **108**, 172405 (2016).

[19] R. Hesse, T. Chassé, R. Szargan. Fresenius J. Anal. Chem. **365**, 48 (1999).

[20] V. Jain, M.C. Biesinger, M.R. Linford. Appl. Surf. Sci. **447**, 548 (2018).

[21] G.S. Grebenyuk, I.A. Eliseev, S.P. Lebedev, E.Yu. Lobanova, D.A. Smirnov, V.Yu. Davydov, A.A. Lebedev, I.I. Pronin. FTT **62**, *3*, 462 (2020) (in Russian).

[22] G.S. Grebenyuk, E.Yu. Lobanova, D.A. Smirnov, I.A. Eliseev, A.V. Zubov, A.N. Smirnov, S.P. Lebedev, V.Yu. Davydov, A.A. Lebedev, I.I. Pronin. FTT **61**, *7*, 1374 (2019). (in Russian).

[23] S.L. Molodtsov, C. Laubschat, G. Kaindl, A.M. Shikin, V.K. Adamchuk. Phys. Rev. B **44**, 8850 (1991).

[24] V.K. Adamchuk, I.V. Lyubinetsky. ZhTF **56**, *9*, 1853 (1986). (in Russian).

[25] I.V. Lyubinetsky. Ozhe-spektroskopiya mezhfazovykh granits blagorodny metall-kremniy. Dis. kand. fiz.-mat. nauk. LGU, L. (1986). (in Russian).

[26] M. Schmitz, L. Kesper, M.G.H. Schulte, P. Roese, U. Berges, C. Westphal. J. Phys.: Condens. Matter **33**, 275001 (2021).

[27] D.K. Sarkar, S. Bera, S. Dhara, S.V. Narasimhan, S. Chowdhury, K.G.M. Nair. Solid State Commun. **105**, *5*, 351 (1998).

[28] Z.J. Pan, L.T. Zhang, J.S. Wu. J. Appl. Phys. **101**, 033715 (2007).

[29] C. Pirri, J.C. Peruchetti, G. Gewinner, D. Bolmont. Solid State Commun. **57**, 361 (1986).

[30] D.Yu. Usachev. Elektronnaya struktura i morphologiya grafena, sintezirovannogo na monokristallicheskikh poverkhnostyakh nikelya i kobalta. Dis. kand. fiz.-mat. nauk. SPbGU, SPb (2010). (in Russian).

[31] C. Riedl, C. Coletti, T. Iwasaki, A.A. Zakharov, U. Starke. Phys. Rev. Lett. **103**, 246804 (2009).

[32] R. Hönig, P. Roese, K. Shamout, T. Ohkochi, U. Berges, C. Westphal. Nanotechnology **30**, 025702 (2019).